Spatial Patterning of the Viscoelastic Core Layer of a Hybrid Sandwich Composite Material to Trigger Its Vibro-Acoustic Performances

Marta Gallo, Corentin Chesnais, Kerem Ege, Quentin Leclere, Nicolas Totaro, R.G. Rinaldi

Spatial patterning of the viscoelastic core layer of a hybrid sandwich composite material to trigger its vibro-acoustic performances

Marta Gallo[1,2], Corentin Chesnais[3,4], Kerem Ege[3,4], Quentin Leclere[3,4], Nicolas Totaro[3,4], Renaud G. Rinaldi[1]

[1] MATEIS - INSA Lyon
[2] IMP - INSA Lyon
[3] LVA - INSA Lyon
[4] CeLyA – Université de Lyon

Abstract

With the aim of decreasing CO_2 emissions, car producers' efforts are focused, among others, on reducing the weight of vehicles yet preserving the overall vibrational comfort. To do so, new lightweight materials combining high stiffness and high (passive) damping are sought. For panels essentially loaded in bending, sandwich composites made of two external metallic stiff layers (skins) and an inner polymeric (i.e. absorbing) core are broadly used. Now aiming at creating materials by design with a better control of the final performance of the part, the tuning of the local material properties is pursued. To this end, the present work focuses on controlling the spatial in-plane viscoelastic properties of the polymeric core of such sandwich structures. The spatial patterning is achieved using a recently developed UV irradiation selective technique of Room Temperature Vulcanization (RTV) silicone elastomeric membrane, in which the ultraviolet (UV) irradiation dose, curing time and temperature are the process parameters controlling the viscoelastic properties of the polymeric membrane. Finally, a protocol for the realization of architected aluminum – silicone – aluminum composite sandwich panels is proposed. The influence of UV irradiation selective technique is demonstrated by Dynamic Mechanical Analysis (DMA) measurements on the silicone core itself and by the Corrected Force Analysis Technique (CFAT) to measure the equivalent Young's modulus and damping of the sandwich structure over a large frequency band. As a first demonstration application, sandwich beams with different core patterns (homogeneous and heterogeneous) are designed and tested. Furthermore, the analytical formalism developed by Guyader *et. al.* is used to model the vibro-acoustic performances of the homogenous sandwich beams and fair model-experiments comparisons are obtained. The spatial patterning of the polymer layer is found to successfully affect the local properties of the composite heterogeneous beam as evidenced by the CFAT method. Finally, this work permits the enunciation of guidelines for designing complex architectured systems with further control of the vibro-acoustics performances.

Introduction

Hybrid composite sandwiches, combining two external metallic layers and an inner constrained viscoelastic core are one of the possible answers to design light material solutions for the transportation industry. Indeed, these material solutions provide high bending stiffness and high damping [1] that are required to, for the least, guaranty the necessary vibro-acoustic performances of the vibrating structure. Several studies investigated numerically and/or experimentally the influence of geometrical and/or material parameters, such as core and metal-skin thickness and composition, on the properties of the composite structure [2-4]. Generally, the polymer layer analyzed in the aforementioned studies is considered to be homogeneous. However, as shown by Unruh [5] with finite element simulations on plate systems, where the mechanical properties of the polymer layer vary with respect to the x,y position within the neutral plane of the plate, the vibro-acoustic behavior of a sandwich panel is strongly affected. Therefore, the local control of the polymer viscoelastic properties offers the opportunity to optimize the vibro-acoustic behavior of the designed structure. Yet, no experimental study can be found on the testing of such architectured hybrid composite structures.

The patterning of stiffness can be achieved by locally altering either or both the local geometry and the local material properties. In this work, with the final objective to design flat panels, and to guaranty good adhesions between the layers, the effort is focused on controlling the local viscoelastic properties of the polymer core layer. For this purpose, we take advantage of a recently published ultraviolet (UV) irradiation selective technique [6]. In details, the UV irradiation of a bar-coated silicone mixture (in presence of an aromatic solvent) leads to the degradation of the catalyst, and ultimately a reduction of the silicone cross-linking rate when submitted to heat cure. Thus, the positioning of a mask between the UV source and the polymer mix can ascertain that the silicone will locally receive different amount of UV doses. By doing so, the cross-linking kinetics can be adjusted spatially. Ultimately, stopping the (heat-cured) reaction before its completion by cooling and/or end-capping the remaining reactive groups will lead to difference in final mechanical properties. Initially developed to modulate the elastic properties of Liquid Silicone Rubber (LSR) silicone membranes, the procedure is now adapted to control the viscoelastic behavior of Room Temperature Vulcanization (RTV) silicone. The crosslinked 3D network results from the similar reaction between vinyl and Si-H sites yet the viscosity is greatly diminished providing enhanced processability.

In this work, with the aim of obtaining sandwich materials, the protocol is further modified to bond the architectured silicone membrane with aluminum thin sheets. Details of the adjusted protocol to design sandwich beams are given in the following section.
Various beams (both homogeneous and heterogeneous) are then obtained and their vibro-acoustics responses are measured. For homogeneous systems, their frequency-dependent flexural behavior is compared with the analytical Guyader model showing good agreement. Finally CFAT method is used to spatially determine the behavior of an architectured sandwich system. All in all, the results evidence the effect of the architecturation of the polymer thin layer on the hybrid sandwich properties.

Materials and Methods

Materials

The rigid skin layers of the sandwich composite were made of 0.3 mm thick (t_{Al}) aluminum sheets. One face was sand-blasted to increase the roughness and favor mechanical adhesion with the polymer thin layer. The sheets were cut down to the correct size (250 mm in length and 25 mm in width) and hot-pressed at 250°C for 1 hour to be flattened out. The viscoelastic core was made of silicone Bluesil™ RTV141 (Bluestar, France). Xylenes (ACS reagent, ≥98.5%, mixture of isomers) were purchased from Sigma-Aldrich and used as received.

The protocol followed to obtain UV-irradiated membrane and/or hybrid architectured sandwich composite consists in four consecutive steps that are depicted in Figure 1. It is worth noting that the aluminum sheets were omitted (and the mold thickness adjusted) to design silicone membranes alone.

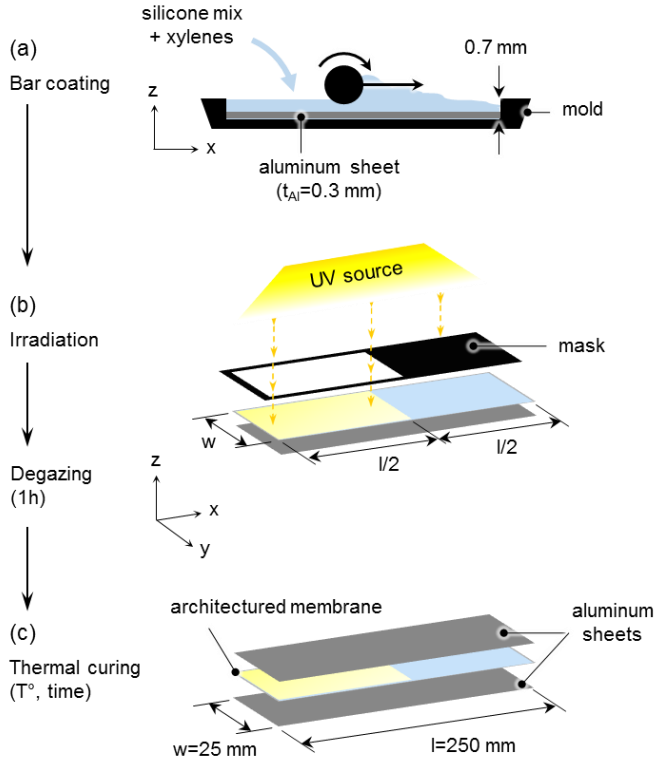

Figure 1: Protocol for obtaining aluminum - architectured silicone - aluminum sandwich. N.B. Homogeneous UV-irradiated silicone membranes are obtained by not using the aluminum sheets and the mask.

First, the two base components were mixed in a weight ratio of 9:1 and with the addition of 10 wt% xylenes. The mixture was molded in a layer less than 0.5 mm thick on top of one aluminum sheet (Figure 1a) and irradiated in a UV Crosslinker CL-1000 (UVP, USA) (Figure 1b). The irradiations were performed at a wavelength λ equal to 254 nm (UVc). The irradiation duration was tuned to control the dose prescribed, with the correspondence between UV durations and doses being verified using a UV radiometer Power Puck II EIT©. Following the irradiation of the silicone mix, the samples were degassed for one hour. Finally, silicone membranes or aluminum – silicone – aluminum sandwiches (≈ 0.5 and 1 mm thick respectively) were obtained by curing the system (irradiated or not) in an oven (Memmert, Germany). The curing time and temperature varied depending on the system prepared. With this protocol, non-irradiated *NIrr* (no irradiation, no mask), irradiated *Irr* (no mask), and half irradiated *NIrr-Irr* (a mask blocking only half of the mold surface) systems were designed. Details on the irradiation and curing steps will be later provided.

Methods

Rheometry tests were performed on the uncured system in order to assess the influence of UV irradiation on the crosslinking kinetics of the RTV silicone. A Physica MCR301 rheometer (Anton Paar, USA) was used for testing with a plan-plan configuration at frequency and strain amplitude of oscillation of 1 Hz and 1% respectively, while applying a temperature dwell (different temperatures were tested, but the heating slope was always equal to 0.7 °C/s).

The viscoelastic properties of the silicone specimens (50 x 10 x 0.5 mm^3) were assessed by Dynamic Mechanical Analyses (DMA) performed on an Eplexor®500N equipment (GABO Qualimeter,

Germany) in tensile mode by applying a tensile strain ε of 1±0.5% for varying temperatures and loading frequencies (1 and 10 Hz).

The high frequency response was evaluated by using the experimental fixture depicted in Figure 2. The beam was fixed onto a rigid frame with an elastic link and excited by a non-contact sensor (MM02). The displacement field was measured with a Polytec PSV-400 scanning laser vibrometer positioned at 2.7 m from the beam. The measurements were performed on a grid of 83 points along the length of the beams and 5 points along the width with a spacing of $\Delta x = \Delta y = 3$mm. The velocity field of the beam was measured on the frequency band [200:1000] Hz in the domain of validity of the applied method.

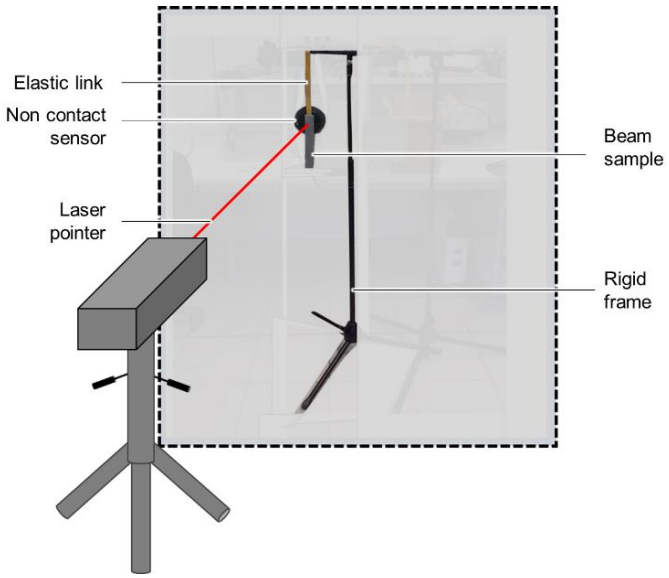

Figure 2: Experimental setup for identifying the equivalent Young's modulus of a beam by CFAT. The beam is fixed onto a rigid frame with an elastic link and is excited by a non-contact sensor (MM02). The velocity field along the length of the beam is measured by a vibrometer with scanning head.

Results and Discussion

Effect of UV dose on the viscoelastic properties of RTV silicone membranes

Figure 3 reports the evolution, as a function of time, of the silicone mix shear modulus (G') when heated at a constant temperature of 80°C. The data were measured by rheometry on two samples submitted to different UV irradiations. Throughout the experiment, the silicone mix reacts, i.e. solidifies. As expected, the moduli increase with time until reaching a plateau value when the material is fully cured, as clearly evidenced for the non-irradiated silicone, with a plateau value of about 0.8 MPa. Also, the irradiation appears to slow down the reaction kinetics and thus the modulus increase, as already demonstrated by Stricher *et. al.* for the case of LSR silicone [6]. When considering the two curves at a specific time-point carefully chosen (e.g., 3000 s in the figure), both materials can be solid and the elastic property difference controlled.

It is worth noting that for hyperelastic entropic materials, the storage modulus is known to be related to the crosslinking density (n) as follow :

$$G' \propto n\,k\,T \quad (1)$$

With k the Boltzmann constant and T the absolute temperature. A lower unsaturated modulus confirms that the network is not fully crosslinked, suggesting that the macromolecular network contains pending and/or free chains with greater mobility, potentially leading to enhanced energy dissipation mechanisms.

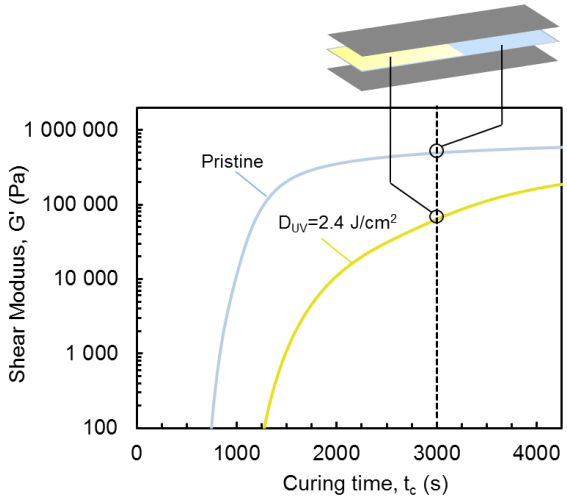

Figure 3: Evolution of the silicone shear modulus as a function of curing time (at 80°C) priory submitted to different UV irradiation conditions. The inset highlights the opportunity to control the difference in the silicone property on a single architectured sandwich composite.

The effect of UV irradiation on the viscoelastic properties of the RTV silicone is investigated using Dynamic Mechanical Analysis in tensile mode. The forced oscillatory deformation is imposed to the sample and the measurement of the associated loading gives access to the complex modulus E^*:

$$E^* = E' + jE'' = E'(1 + j\eta) \quad (2)$$

where E' is the storage modulus (also depicted as the Young's modulus) and E'' the loss modulus. $\eta = \tan\delta = E''/E'$ corresponds to the loss factor and quantifies the amount of energy dissipated by the sample. Figure 4 displays the temperature and frequency dependent response of the non-irradiated fully cured RTV silicone (corresponding to the pristine sample in Figure 3). The silicone was cured for 2h at 150°C as recommended by the technical data sheet [7]. The storage modulus is seen to linearly increase with increasing temperature as suggested by Equation 1. For a given temperature, both the storage modulus and loss factor increase with increasing frequency. Yet, the loss factor remains below 5% within the experimental conditions covered and the modulus exhibits a very small variation (few percents) confirming that the fully cured RTV silicone is mostly hyperelastic. It is worth noting that the magnitude of the storage modulus E' is consistent with the plateau value of the shear modulus G' reported in Figure 3. Indeed, isotropic hyperelastic materials are known to deform with no volume change (the Poisson ratio $\nu \approx 0.5$), so that the tensile Young's modulus is about three times greater than the shear modulus ($E' = G'2(1+\nu) \approx 3G'$) [8].

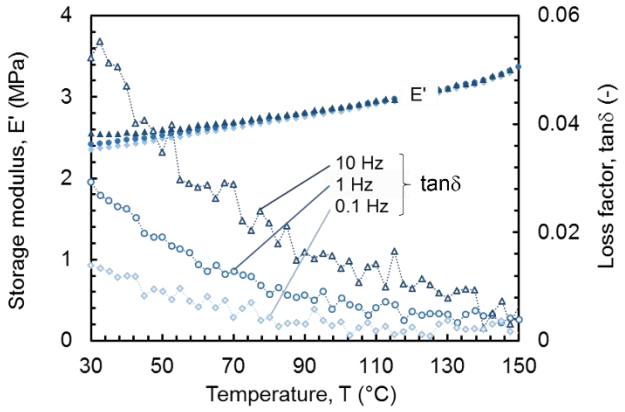

Figure 4: Viscoelastic properties of the pristine silicone membrane as a function of temperature and loading frequency.

Now focusing on the effect of UV irradiation, DMA were performed at room temperature and two frequencies (1 and 10 Hz) on silicone coupons that were cured for 30 minutes at 80°C after being irradiated. The curing conditions were chosen accordingly to the aforementioned rheometry results (see Figure 3) so that significant difference in the viscoelastic properties can be seen as a function of the irradiation dose.

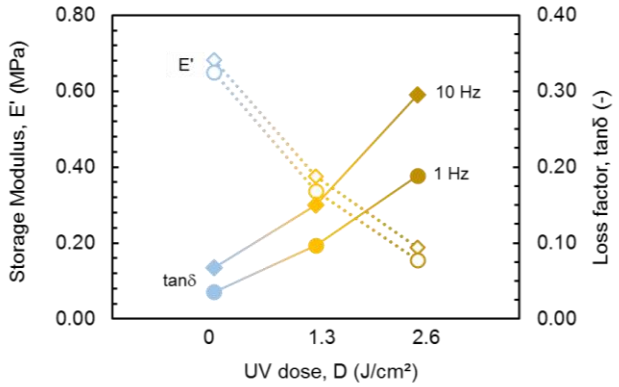

Figure 5: Room temperature viscoelastic properties of silicone membranes as a function of UV irradiation and loading frequency.

The results are presented in Figure 5 where the storage modulus *E'* and the loss factor tanδ are displayed as a function of the UV dose. The storage modulus decreases and the dissipation increases, both mostly linearly, with increasing the irradiation dose. More precisely, after receiving a UV dose of 2.6 J/cm² the modulus is divided by 3 and the loss factor multiplied by 5. Whatever the dose, the moduli remain below the modulus reported in Figure 3, confirming that the silicones are not fully cured. Yet, since the greater the UV irradiation the slower the crosslinking kinetics, irradiated silicones exhibit enhanced dissipative viscoelastic behavior. This is further evidenced by the frequency dependence of E' and tanδ which both increase with increasing UV irradiation.

Apparent Young's modulus and damping of homogeneous three-layered plates

Knowing the variability of the silicone viscoelastic properties when submitted to UV irradiations prior to thermal curing, the prediction of the large frequency response of homogenenous aluminum – silicone – aluminum sandwiches is achieved using the analytical model by Guyader [9,10]. This model together with two other formalisms (*Ross-Kerwin-Ungar* model and *Lamb waves* model) have been recently compared to experiments performed on steel-polymer-steel multilayer plates and very good agreement for the whole [40 Hz - 20 kHz] frequency band was obtained [11, 12]. In brief, the Guyader model allows for the determination of the equivalent (or "apparent") single layer plate complex bending stiffness (D^*_{eq}) as a function of the loading frequency (*f*):

$$D^*_{eq}(f) = D_{eq}(f)(1 + j\,\eta_{eq}(f)) \qquad (3)$$

The calculation of D^*_{eq} is based on the Love-Kirchhoff thin plate theory and deduces the property of a single layer plate that replicates the transverse displacement of the multilayer (sandwich) plate. The analytical method applies the travelling wave approach to a simplified multilayer model (where membrane and shear effects are considered for each layer). Continuity conditions (displacement and shear stresses) at each layer interface are used to obtain the equation of motion of the multilayer plate field expressed as a function of the first layer field.

The density (ρ_{eq}) and Poisson ratio (ν_{eq}) of the equivalent homogeneous material are straightforwardly computed from the dimensions and properties of the constitutive layers:

$$\rho_{eq} = \frac{\sum_i h_i \rho_i}{h} \qquad (4)$$

$$\nu_{eq} = \frac{\sum_i h_i \nu_i}{h} \qquad (5)$$

Where $h = \sum_i h_i$ is the total thickness of the composite panel, and the subscripts "eq" and "i" refer to the parameters of the equivalent homogenized material and of the i^{th} layer of the multilayer material, respectively.

Finally, the frequency-dependent equivalent homogeneous Young's modulus (E_{eq}) and loss factor (η_{eq}) are calculated from the value of the equivalent complex bending stiffness (D^*_{eq}):

$$E_{eq}(f) = \Re\left(D^*_{eq}(f)\right)\frac{12\left(1-\nu^2_{eq}\right)}{h^3} \qquad (6)$$

$$\eta_{eq}(f) = \frac{\Im\left(D^*_{eq}(f)\right)}{\Re\left(D^*_{eq}(f)\right)} \qquad (7)$$

Figure 6 displays the wide frequency equivalent modulus and loss factor of two infinite sandwich structures. The two systems have prescribed thicknesses with varying silicone properties to mimic the effect of UV irradiation. Thus, *Irr* and *NIrr* refer to Irradiated and Non-Irradiated silicone membranes respectively and the material properties assigned are of the order of the experimental values reported in Figure 4 and 5.

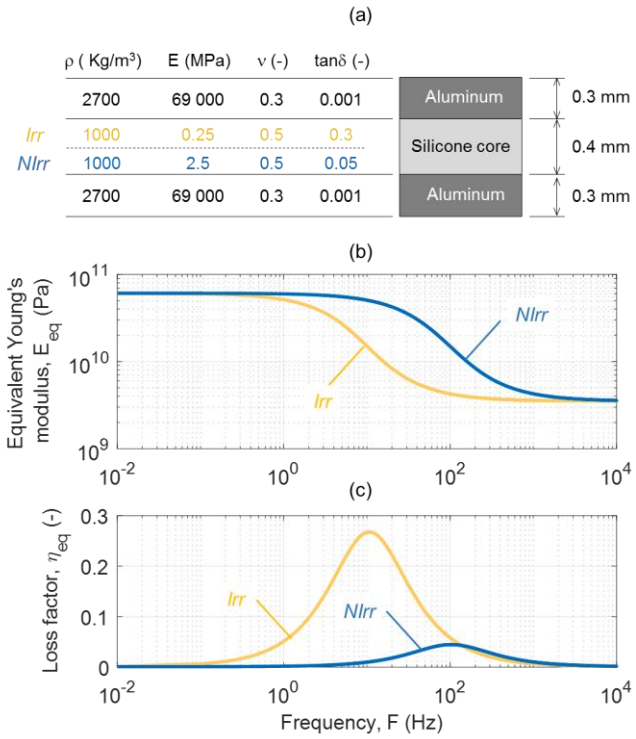

Figure 6: Analytical prediction of the large-frequency band properties of an aluminum – silicone – aluminum sandwich structure. (a) Input parameters. Frequency dependence of (b) the Equivalent Young's modulus and (c) the loss factor.

Focusing on a given sample, the observed behavior is typical of constrained-layer damping sandwich plates:

- Equivalent Young's modulus (E_{eq}): a constant value (high rigidity) at low frequency decreasing gradually (on the *transition* zone governed by shearing of the constrained layer) to a lower asymptotic value at high frequencies.

- Equivalent loss factor (η_{eq}): limited damping at low and high frequencies (close to the loss factor value of the metallic skin), and high damping for a limited frequency range where the shearing of the highly-damped constrained core layer is maximum (*optimum shearing zone*).

Now focusing on the effect of the silicone properties caused by UV irradiation, it is worth noting that the low and high frequency responses are equivalent. In fact, at low frequency, the asymptotic value of the equivalent rigidity is equal to the flexural rigidity of a panel with rigidly interconnected structural skin components and thus does not depend on the material properties of the silicone core layer. Similarly the high frequency response is simply equal to the sum of the flexural rigidities of the structural components (as if they were not interconnected), meaning that the contribution of the compliant core layer is also negligible. Yet, the modulus decrease of the *Irr* (more compliant) sandwich occurs at lower frequency, almost a decade earlier compared to the *NIrr* system. Furthermore, the dissipation of the *Irr* (more viscoelastic with higher η_{sil}) sandwich is increased in the "optimum shearing zone". Hence, the silicone layer viscoelastic properties result in a frequency shift of the optimal shearing zone of the sandwich structure (towards low frequency when the silicone stiffness decreases). Naturally, in this regime the dissipation is directly governed by the silicone dissipative properties and is thus more pronounced.

In the light of the aforementioned explanation, the high frequency equivalent modulus and the "optimum shearing" zone strongly depends on the sample's thickness. It is further demonstrated in Figure 7 where the silicone thickness of the *Irr* configuration is decreased from 0.4 to 0. 05 mm, while the thicknesses of the aluminum layers remain equal to 0.3 mm. With the decrease of the polymer thickness, and thus its volume fraction, the shearing zone is shifted towards higher frequency and its amplitude decreases, mostly because the diminished thickness leads to a major increase of the high frequency modulus.

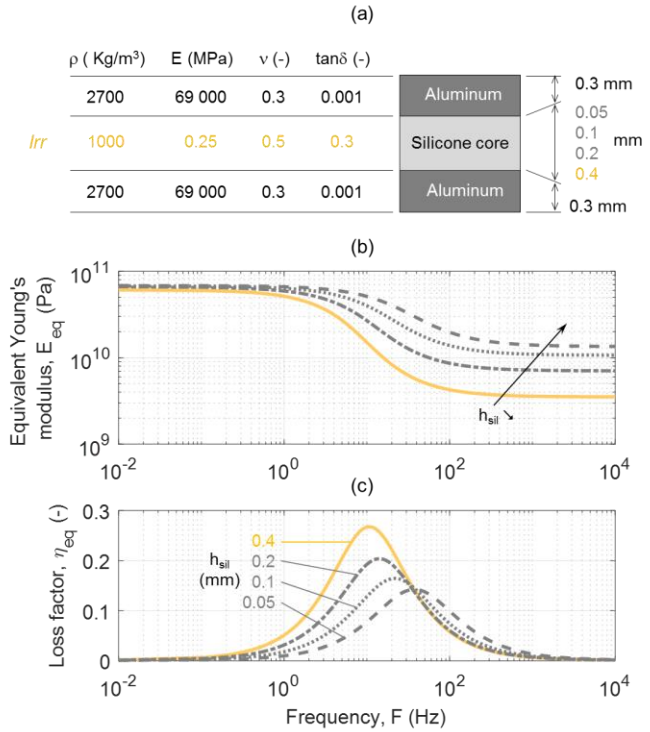

Figure 7 : Effect of the silicone layer thickness on the large-frequency band properties of an aluminum – silicone – aluminum sandwich structure (a) Input parameters, (b) Equivalent Young's modulus and (c) loss factor as a function of frequency.

It is worth mentioning that the validity of the model of Guyader is limited to frequencies where no out-of-phase flexural motion of the skins exists. Focusing on the less favorable case composed of the thicker silicone layer (0.4mm), the first "breathing mode" occurs at about 6.2 kHz (see [11] for description of the analytical prediction of the breathing mode) which falls above the experimental [10Hz - 2kHz] frequency domain of interest. Nevertheless, other models may be used for very thick laminated panels or highly damped laminate composites such as the General Laminate model [13]. The reader could also refer to the work of Carrera [14] where several models are compared.

Identification of frequency-dependent equivalent Young's modulus of a hybrid composite beam

Following the protocol depicted in Figure 2 and driven by the results presented in the previous paragraph, three hybrid composite beams were prepared:

- *NIrr*: No irradiation was applied to the silicone and the beam was heat-cured for 2h at 150°C,
- *Irr*: A UV dose of 2.6 J/cm² was applied to the sample prior to a curing step of 30 min at 80 °C,
- *NIrr-Irr*: A UV dose of 2.6 J/cm² was applied to half of the beam sample prior to a curing step of 30 min at 80 °C,

The beams were about 1 mm thick (±10%) so that the average thickness of the silicone layers h_{sil} was about 0.4 mm. When referring to the aforementioned experimental characterization, the expected (theoretical) material properties of the aluminum and silicone layers of the three beams are recalled in Table 1 below.

Table 1: Expected mechanical properties of the aluminum and silicone layers used in the three hybrid composite beams.

	Beam NIrr	Beam Irr	Beam NIrr-Irr NIrr	Beam NIrr-Irr Irr	Al
Density ρ_{sil} (kg/m^3)	1000				2700
Young's modulus E_{sil} (MPa)	2.5	0.25	0.7	0.25	69000
Loss factor η_{sil} (-)	0.05	0.3	0.1	0.3	0.001
Poisson ratio ν_{sil} (-)	0.5				0.3

The frequency-dependent equivalent Young's modulus E_{eq} of the beam was then spatially resolved using the Corrected Force Analysis Technique. This method has been firstly introduced to identify the force distribution acting on a flat structure (beam or plate) [15]. It is based on the approximation of the equation of motion of the structure by a finite difference scheme. In the case of flexural beams, the equation of motion at the angular frequency ω writes:

$$EI\frac{\partial^4 w}{\partial x^4}(x) - \rho S\omega^2 w(x) = p(x) \qquad (7)$$

where E, I, ρ and S are respectively the Young's modulus, the flexural moment of inertia, the density and the surface of the cross section. w(x) is the displacement in meters and p(x) is the force distribution in N/m applied to the beam.

As can be seen in Eq. (7), the right hand side member can be directly assessed from the experimental estimation of the left hand side member. The fourth derivative in Eq. (7) can be approximated by a centered finite difference scheme:

$$\frac{\partial^4 w}{\partial x^4}(x) \approx \delta_\Delta^{4x} = \frac{w(x-2\Delta) - 4w(x-\Delta) + 6w(x) - 4w(x+\Delta) + w(x+2\Delta)}{\Delta^4} \qquad (8)$$

where Δ is the spacing between two consecutive points of the experimental grid line defined along the length of the beam. The force distribution is then directly estimated from the displacement measured at 5 positions around the identification point as presented in Figure 8.

This approach, known as FAT, is local (information needed on the finite difference scheme only) and does not depend on boundary conditions of the structure. However, this approach is highly disturbed by measurement noise and a filtering step is mandatory. This filtering can be achieved easily by adjusting the step of the scheme at nΔx, so as to optimize its size as a function of the natural wavelength of the beam [16]. However, in this case a corrected version of the FAT technique (CFAT) has to be implemented so as to reduce the bias error.

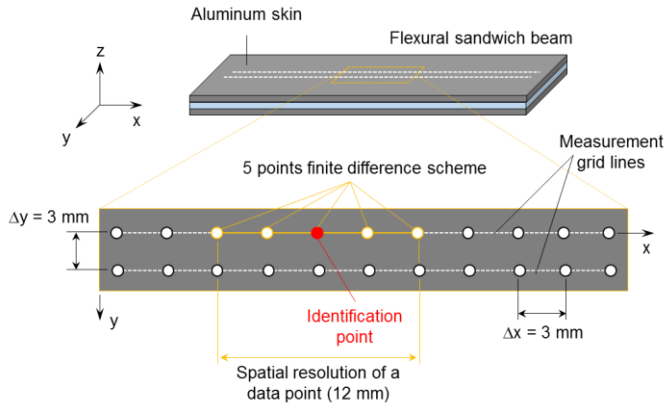

Figure 8: Illustration of the 5 points of the finite difference scheme with in FAT. The scheme is moved along the length of the beam to identify the spatial variations of force distribution.

The corrected FAT estimation of the force distribution is finally given by:

$$p^{CFAT}(x) = EI\mu^4\delta_\Delta^{4x} - \rho S\omega^2 w(x) \qquad (9)$$

where

$$\mu = \frac{k_N\Delta}{\sqrt{2-2\cos(k_N\Delta)}} \qquad (10)$$

k_N is the flexural wavenumber of the beam, $k_N = \sqrt[4]{\frac{\rho S}{EI}\omega^2}$.

If the force distribution is null in the zone scanned by the finite difference scheme, Eq. (9) becomes [16]:

$$\frac{EI}{\rho S} = \omega^2\Delta^4\left[\operatorname{acos}\left(1 - \frac{\Delta^2}{2}\sqrt{\frac{\delta_\Delta^{4x}}{w(x)}}\right)\right]^{-4} \qquad (11)$$

If I, ρ and S are considered to be known, the Young's modulus can be estimated locally and at a particular angular frequency ω. This approach can be then an experimental method to evaluate the spatial variation of the Young's modulus (by moving the finite difference scheme) as well as its frequency dependency.

However, one has to pay attention to the fact that the equation of motion (7) used in this method is only valid for a homogeneous isotropic material. In case of a beam made of a non-homogeneous and/or non-isotropic material (composite material, sandwich panels, polymer reinforced with short glass fibers for example), CFAT gives access to an equivalent homogeneous isotropic Young's modulus as a function of frequency [17].

First, to evaluate how CFAT method can be used to quantify the equivalent Young's modulus of a hybrid composite beam as a function of frequency, the method was applied on the two *NIrr* and *Irr* beams. Since these beams are spatially homogeneous, a spatial averaging was applied to obtain the results plotted in Figure 9. The identified equivalent Young's moduli are compared to the analytical model predictions plotted in Figure 6(b). Since the (high frequency) equivalent modulus strongly depends on the core thickness, predictions obtained with slightly modified silicone thickness $h_{sil} = 0.35$ mm were added to the plot.

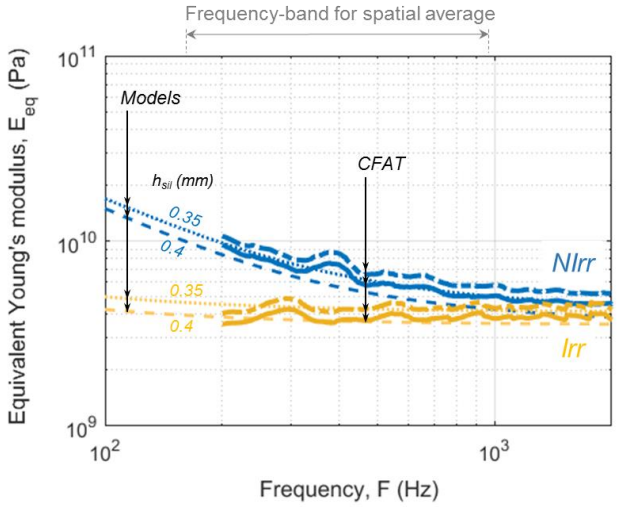

Figure 9: Equivalent Young's modulus of the *NIrr* (blue) and *Irr* (orange) beams as a function of frequency using CFAT (thick lines) and analytical predictions from the Guyader model (thin lines). Two silicone thicknesses $h_{sil} = 0.4$ and $h_{sil} = 0.35$ mm are employed to evidence the importance of controlling the polymer core thickness.

The CFAT measurements evidence the difference of equivalent modulus, between *NIrr* and *Irr* beams, the former being greater. More importantly, the measured profiles coincide with the analytical model. Nevertheless, and as already pointed out, it is worth noting that the thickness of the silicone layer is of great importance. Indeed, as shown in Figure 9, the discrepancies between experimental measurements and theoretical predictions are strongly diminished when the silicone layer thickness is decreased by as few as 50 microns, suggesting that the set-up should be carefully set.

Furthermore, it should to be also pointed out that the equivalent Young's modulus of the *Irr* beam exhibits a slight increase with increasing frequency. This behavior is not captured by the analytical model, since the Young's modulus of the silicone layer is set to be constant. Yet, the results in Figure 5 suggest that the Young's modulus of the (irradiated but not only) silicone increases with increasing frequency, which ultimately would result in a slight increase of the equivalent Young's modulus of the sandwich composite. This point will be further studied as frequency dependent modulus of the silicone can be determined (and implemented) as a function of the UV irradiation dose (master curves construction).

Finally, the effect of spatial patterning has been evaluated on the equivalent Young's modulus identified by CFAT for the three beams, and successfully replicated using another data reduction methodology depicted in [18]. The results presented in Figure 10 are frequency averaged on the frequency band [150-950] Hz as highlighted in the upper Figure 9. The evolutions of the Young's moduli along the length of each beam show that the patterning (half of the beam not irradiated, half of the beam irradiated) is effective. The modulus of the *Irr - NIrr* architectured beam falls well within the values measured for the *NIrr* and *Irr* homogeneous beams. Let's point out that the equivalent modulus within the *NIrr* region should be lower than the one measured for the *NIrr* beam since the curing step of the architectured beam is such that the crosslinking is not completed (see Table 1). That being said, the heat transfer differs between the rheometer and the furnace, so that it is important to consider the values in Table 1 as theoretical.

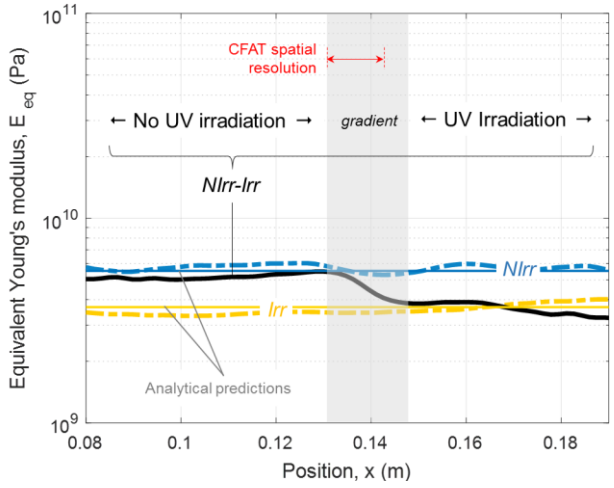

Figure 10: Equivalent Young's modulus of the hybrid sandwich beams as a function of the position along the beam using CFAT. For the heterogeneous *NIrr-Irr* beam, the graded region is highlighted and coincide with the vicinity of the mask's edge.

Also, the transition between the *NIrr* and *Irr* regions corresponding to the grey zone in Figure 10 is quite sudden (less than 2 cm), yet greater than the spatial resolution of the CFAT measurements. Thus, the CFAT is well adapted and evidence that the selective UV irradiation of the silicone layer is efficient to locally modify the mechanical property of sandwich composite. Again, the variation observed on the Young's modulus of the *Nirr* beam is most likely due to the spatial variations in the thickness of the silicone layer.

Conclusions

A protocol is developed to design lightweight aluminum – silicone – aluminum sandwich structures with spatial control of the viscoelastic properties of the polymeric core. The tuning is obtained by selective UV irradiation of the silicone layer. The UV irradiation is applied onto the silicone mix prior to thermal curing and the irradiation is seen to decrease the crosslinking kinetics of the silicone material. Consequently, under controlled thermal curing conditions, the irradiated silicone exhibits lower modulus and greater damping properties compared to non-irradiated one. Following this protocol, sandwich beams were designed and their spatial and frequency dependent properties (equivalent Young's modulus) successfully characterized using CFAT.

Homogeneous beams were prepared with varying silicone properties using UV irradiation. The measured properties fall well within the analytical predictions using the analytical Guyader model, yet further confirming the validity of using CFAT to determine the structure's equivalent properties. As a consequence to UV irradiation, the

equivalent modulus drop corresponding to the optimum shearing zone is seen to shift towards lower frequency and be more dissipative.

CFAT is also applied onto a heterogeneous beam in which only one half has been irradiated. The feasibility of spatial patterning using UV irradiation on silicone layer is demonstrated as spatial evolution of the equivalent modulus is clearly evidenced.

Finally, The UV dose can be used to tune the property of the silicone layer in order to adjust the vibro-acoustic performances of a flat sandwich beam or panel. Considering the analytical predictions and the associated frequency shift of the "maximum shearing zone" of a homogeneous sandwich composite in which the polymer contribution to the overall composite response is maximum, the explored material solutions could be dedicated from low to very low frequency ranges where meta-material-based solutions are often inefficient. Further studies now focus on the effect of the viscoelastic patterning on the "optimum shearing zone" (position and width) and aim at considering the intrinsic frequency-dependent properties of the silicone material.

References

1. Li, Z., and Crocker, M. J., "A review on vibration damping in sandwich composite structures," *International Journal of Acoustics and Vibration*, *10*(4):159-169, 2005.
2. Irazu, L., and Elejabarrieta, M. J., "The effect of the viscoelastic film and metallic skin on the dynamic properties of thin sandwich structures," *Composite structures*, 176:407–419, 2017.
3. [6] Y. Swathi, Y., and Abdul Kalam, S., "Sandwich Treatment In FRP Beams: Static And Dynamic Response," *International Journal of Engineering Research and Technology*, 1(9):2278, 2012.
4. Grewal, J. S., Sedaghati, R., and Esmailzadeh, E., "Vibration analysis and design optimization of sandwich beams with constrained viscoelastic core layer," *Journal of Sandwich Structures & Materials*, 15(2):203–228, 2013.
5. Unruh, O., "Influence of inhomogeneous damping distribution on sound radiation properties of complex vibration modes in rectangular plates," *Journal of Sound and Vibration*, 377:169–184, 2016.
6. Stricher, A., Rinaldi, R. G., Machado, G., Chagnon, G., et al., "Light-Induced Bulk Architecturation of PDMS Membranes," *Macromolecular Materials Engineering*. 301(10):1151-1157, 2016.
7. https://www.benam.co.uk/uploads/tds/RTV141-TDS.pdf, December 2017
8. Stricher, A. M., Rinaldi, R. G., Barrès, C., Ganachaud, F., et al., "How I met your elastomers: from network topology to mechanical behaviours of conventional silicone materials," *RSC Advances*, *5*(66):53713-53725, 2015.
9. Guyader J.L., Lesueur C., "Acoustic transmission through orthotropic multilayered plates, part I: plate vibration modes", *Journal of Sound and Vibration* 58(1):51-58, 1978.
10. Guyader J.L., Cacciolati C., "Viscoelastic properties of single layer plate material equivalent to multi-layer composite plate", in: *Proceedings of Inter-Noise*, Istanbul, Turkey, 2007.
11. Ege K., Henry V., Leclère Q., Rinaldi R.G., Sandier C., "Vibrational behavior of multilayer plates in broad-band frequency range: comparisons between experimental and theoretical estimations", in: *Proceedings of Inter-Noise*, San Francisco, USA, 2015.
12. Ege K., Roozen B., Leclère Q., Rinaldi R.G., "Assessment of the apparent bending stiffness and damping of multilayer plates; modelling and experiment", submitted to *Journal of Sound and Vibration.*
13. Ghinet, S., Atalla, N., "Modeling thick composite laminate and sandwich structures with linear viscoelastic damping", *Computers & Structures*, 89:1547-1561, 2011.
14. Carrera E., "An assessment of mixed and classical theories on global and local response of multilayered orthotropic plates", *Composite structures*, 50(2):183-198, 2000.
15. Leclère, Q., Pézerat, C., "Vibration source identification using corrected finite difference schemes", *Journal of Sound and Vibration*, 331(6):1366–1377, 2012.
16. Leclère, Q., Ablitzer, F., Pezerat, C., "Identification of loads of thin structures with the corrected Force Analysis technique: An alternative to spatial filtering regularization" *Proceedings of ISMA 2014*, Leuven, Belgium, 2014.
17. Leclère, Q., Ablitzer, F., Pézerat, C., "Practical implementation of the corrected force analysis technique to identify the structural parameter and load distributions", *Journal of Sound and Vibration*, 351:106–118, 2015.
18. Wassereau, T., Ablitzer, F., Pézerat, C., Guyader, J. L., "Experimental identification of flexural and shear complex moduli by inverting the Timoshenko beam problem", *Journal of Sound and Vibration*, 399:86-103, 2017.

Acknowledgments

This work has been funded by the French Carnot Institute network "Ingénierie@Lyon" (Mhyriam Project).
This work was performed within the framework of the Labex CeLyA of Université de Lyon, operated by the French National Research Center Agency (ANR-10-LABX-0060/ ANR-11-IDEX-0007)